Supporting Information of

Fluorinate a Polymer Donor through Trifluoromethyl Group for High-Performance Polymer Solar Cells

Chao Yao, Yanan Zhu, Kaichen Gu, Jiajun Zhao, Jiaoyi Ning, Dmitrii F. Perepichka, Yueh-Lin Loo, Hong Meng *

C. Yao, Y. N. Zhu, J. J. Zhao, J. Y. Ning, Prof. H. Meng
School of Advanced Materials
Peking University Shenzhen Graduate School
Shenzhen, 518055, China
E-mail: menghong@pku.edu.cn

K. Gu, Prof. Y.-L. Loo
Department of Chemical and Biological Engineering
Princeton University
Princeton, New Jersey 08544, United States

Prof. Y.-L. Loo
Andlinger Center for Energy and the Environment
Princeton University
Princeton, New Jersey 08544, United States

Prof. D.-F. Perepichka
Department of Chemistry and Centre for Self-Assembled Chemical Structures
McGill University
801 Sherbrooke Street West, Montreal, H3A0B8, QC, Canada.

Experimental Section

1. Materials and synthesis

The monomer 2,6-bis(trimethyltin)-(4,8-bis(5-(2-ethylhexyl)thiophen-2-yl)-benzo[1,2-*b*:4,5-*b*′]dithiophene (BDT-Sn) was purchased from SunaTech Inc. 2,5-Dibromothiophene-3-carboxylic acid was synthesized according to previously-reported procedures[1]. All other chemical reagents were used as received.

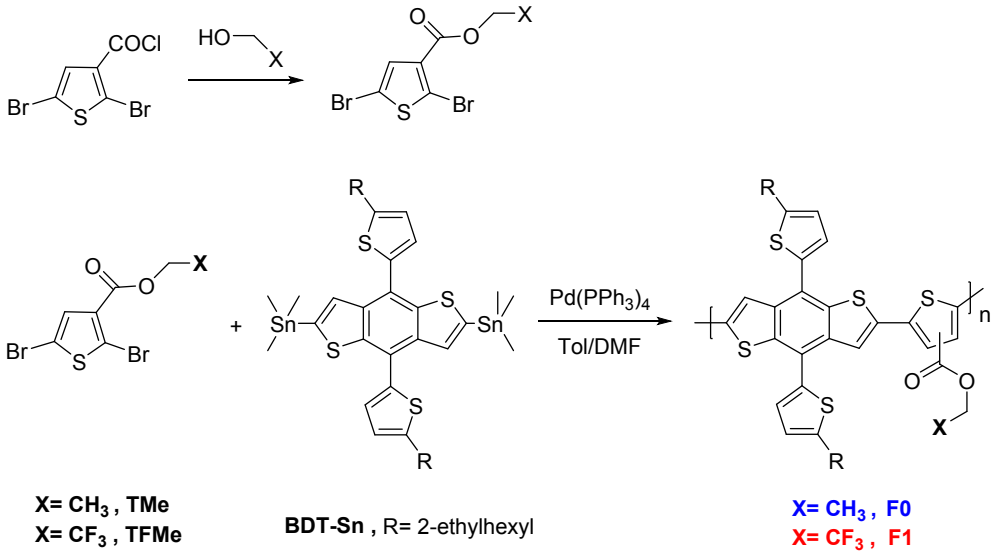

Figure S1. Synthesize route of monomers and polymers.

Ethyl-2,5-dibromothiophene-3-carboxylate (TMe)

2,5-Dibromothiophene-3-carboxylic acid (1.5 g, 0.005 mol) and 15 mL of $SOCl_2$ were refluxed for 6 h, and the excess $SOCl_2$ was removed under vacuum. A light yellow low-melting solid was obtained. Then, 20 mL ethyl alcohol and 1 mL of dry pyridine were added to the flask dropwise through an addition funnel. The mixture was stirred for 6 h at 40 °C, cooled, poured into a mixture of 15 g of ice and 20 mL of 1 M HCl, and stirred. The solution was washed with ether (4 × 50 mL), and the organic phase was washed with saturated $NaHCO_3$ (3 × 50 mL) and dried K_2CO_3. The ether was removed with a rotary evaporator, and a light yellow crude product was obtained. The crude product was further purified by column chromatography on silica gel to give TMe as white solid (1.3 g, 78% yield). **^{1}H-NMR** (300 MHz, Chloroform-d): δ 7.36 (s, 1H), 4.34 (q, J = 7.2 Hz, 2H), 1.38 (t, J = 7.1 Hz, 3H). **MS** (MALDI-TOF): calculated for $C_7H_6Br_2O_2S$ [M^+], 311.852; found: 311.330.

2,2,2-trifluoroethyl-2,5-dibromothiophene-3-carboxylate (TFMe)

2,5-Dibromothiophene-3-carboxylic acid (1.5 g, 0.005 mol) and 15 mL of $SOCl_2$ were refluxed for 6 h, and the excess $SOCl_2$ was removed under vacuum. A light yellow low-melting-point solid was obtained. Then, 20 mL dichloromethane, 2mL CF_3CH_2OH and 1 mL of dry pyridine were added to the flask dropwise through an addition funnel. The mixture was stirred for 6 h at 40 °C, cooled, poured into a mixture of 15 g of ice and 20 mL of 1 M HC1, and stirred. The solution was washed with ether (4 x 50 mL), and the organic phase was washed with saturated $NaHCO_3$ (3 x 50 mL) and dried K_2CO_3. The ether was removed with a rotary evaporator, and a light yellow crude product was obtained. The crude product was further purified by column chromatography on silica gel to give TFMe as white solid (1.4 g, 80% yield). ^{1}H-NMR (300 MHz, Chloroform-d): δ 7.39 (d, J = 1.5 Hz, 1H), 4.65 (q, J = 8.3 Hz, 2H). **MS** (MALDI-TOF): calculated for $C_7H_3Br_2F_3O_2S$ [M^+], 365.824; found: 365.565.

F0

TMe (0.0314 g, 0.1 mmol) and BDT-Sn (0.090 g, 0.1 mmol) were dissolved into 6 mL of toluene/DMF(volume ratio 5/1) in a two-neck round-bottom flask. The solution was flushed with

argon for 5 min, and 5 mg of $Pd(PPh_3)_4$ was added into the flask subsequently. The mixture was flushed with argon for another 15 min and then allowed to stir at 110°C for 20h under an argon atmosphere. Then, the reactant was cooled down to room temperature, and the polymer was precipitated into 100 mL of methanol. The polymer was collected by filtration and further purified by Soxhlet extraction using a variety of organic solvents (acetone, hexane and chloroform). The polymer was precipitated again in 100 mL of methanol and obtained as crimson solid with a yield of about 60%.

F1

TFMe (0.0368 g, 0.1 mmol) and BDT-Sn (0.090 g, 0.1 mmol) were dissolved into 6 mL of toluene/DMF(volume ratio 5/1) in a two-neck round-bottom flask. The solution was flushed with argon for 5 min, and 5 mg of $Pd(PPh_3)_4$ was added into the flask subsequently. The mixture was flushed with argon for another 15 min and then allowed to stir at 110°C for 24h under an argon atmosphere. Then, the reactant was cooled down to room temperature, and the polymer was precipitated into 100 mL of methanol. The polymer was collected by filtration and further purified by Soxhlet extraction (acetone, hexane and chloroform). The polymer was precipitated again in 100 mL of methanol and obtained as brown solid with a yield of about 70%.

2. Measurements and Instruments

The NMR spectra were measured using Bruker AVANCE 300 or 400 or 500 MHz spectrometer. Mass spectra were measured on a Bruker Daltonics Biflex III MALDI-TOF Analyzer in the MALDI mode. Solution (CB) and thin film (on a quartz substrate). UV-vis absorption spectra were recorded using a JΛSCO V-570 spectrophotometer. Electrochemical measurements were carried out under nitrogen in a solution of tetra-n-butylammonium hexafluorophosphate ($[nBu_4N]+[PF_6]–$) (0.1 M) in CH_3CN employing a computer-controlled CHI660C electrochemical workstation, glassy carbon working electrode coated with donor films, an Ag/Ag^+ reference electrode, and a platinum-wire auxiliary electrode. The potentials were referenced to a ferrocenium/ferrocene ($FeCp^{2+}/0$) couple using ferrocene as an internal standard. Atomic force microscopy (AFM) was performed using Multimode 8 atomic force microscope in tapping mode. Space charge limited current (SCLC) mobility was measured using a diode configuration of ITO/PEDOT:PSS/donor:acceptor/MoO_3/Ag for hole mobility and ITO/ZnO/donor:acceptor/PFNBr/Al for electron mobility and fitting the results to space charge limited form, where SCLC equation is described by :

$$J_{SCLC} = \frac{9}{8}\varepsilon_o \varepsilon_r \mu_o \frac{V^2}{L^3}$$

where J is the current density, L is the film thickness of the active layer, μ_0 is the charge mobility, ε_r is the relative dielectric constant of the transport medium, ε_0 is the permittivity of free space (8.85×10^{-12} F m^{-1}), V is the internal voltage in the device (= V_{appl} - V_{bi}), where V_{appl} is the voltage applied to the device and V_{bi} is the built-in voltage due to the relative work function difference of the two electrodes (V_{bi} = 0.23 V here).

GIWAXS measurements were performed at the Complex Materials Scattering (CMS) beamline of the National Synchrotron Light Source II (NSLS-II), Brookhaven National Lab. The X-ray beam with an energy of 13.5 keV shone upon the samples with the incident angle of 0.1° with respect to the substrate between the critical angles of the organic film and the Si substrate. A custom-made

Pilatus-800K detector was placed at the distance of 257 mm from the sample center to capture GIWAXS images with the exposure time of 10 s. All GIWAXS images have been background subtracted.

3. Organic solar cell fabrication

The devices were fabricated with a structure of glass/ITO/ZnO/donor:acceptor/ MoO_3/Ag. The ITO-coated glass substrates were cleaned by ultrasonic treatment in detergent, deionized water, acetone, and isopropyl alcohol under ultra-sonication for 15 minutes each and subsequently dried by a nitrogen blow. ZnO electron transport layer was prepared onto the ITO glass through spin coating at 3000 rpm from a ZnO precursor solution, then the ZnO substrates were immediately baked in air at 200 ℃ for 30 min, the substrates were transferred into an argon-filled glove box. Subsequently, the active layer was spin-coated from the blend chlorobenzene solutions of donor and acceptor. The MoO_3 layer (ca. 10 nm) and Ag (ca. 80 nm) were successively evaporated onto the surface of the photoactive layer under vacuum (ca. 10^{-6} Pa). The current density-voltage (J-V) curves of photovoltaic devices were obtained with a Keithley 2400 source-measure unit. The photocurrent was measured under illumination simulated AM 1.5G (100 mW cm^{-2}) irradiation using a SAN-EI XES-70S1 solar simulator, calibrated with a standard Si solar cell. External quantum efficiencies were measured using Stanford Research Systems SR810 lock-in amplifier. The active area of the device was ca. 4.5mm^2.

4. DFT Calculations

The equilibrium geometry of the polymer donors were optimized at B3LYP/6-31G(d,p) level of theory in the gas phase and the alkyl side-chains of BDT were replaced by hydrogen for simplification. Dipole moments were calculated at PBE0/def2-TZVP level according to the benchmark work of Hait et al.[2] All the calculations were carried out in Gaussian 09 (ver. D.01) package.

5. Figures and tables

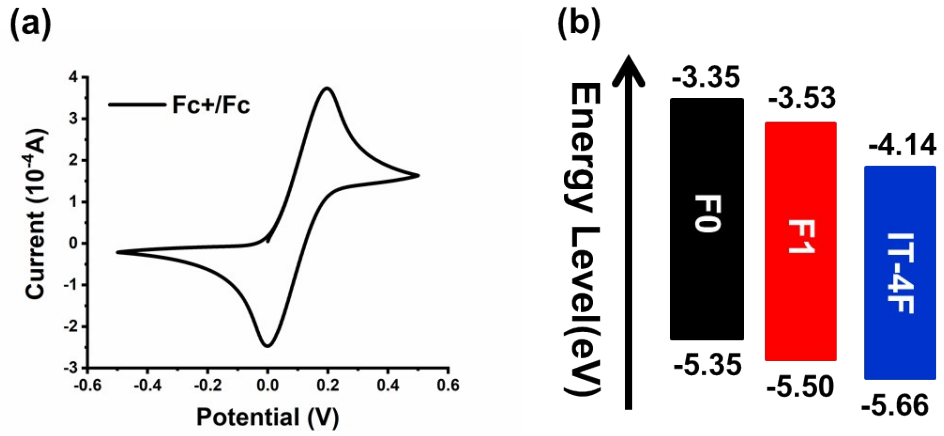

Figure S2. (a) Cyclic voltammetry measurements of ferrocene in CH_3CN. (b) Energy levels of F0, F1 and IT-4F.

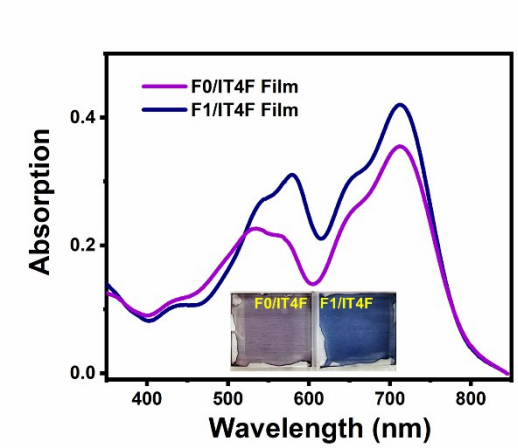

Figure S3. UV-vis absorption of F0/IT-4F and F1/IT-4F blend films with thickness around 100 nm.

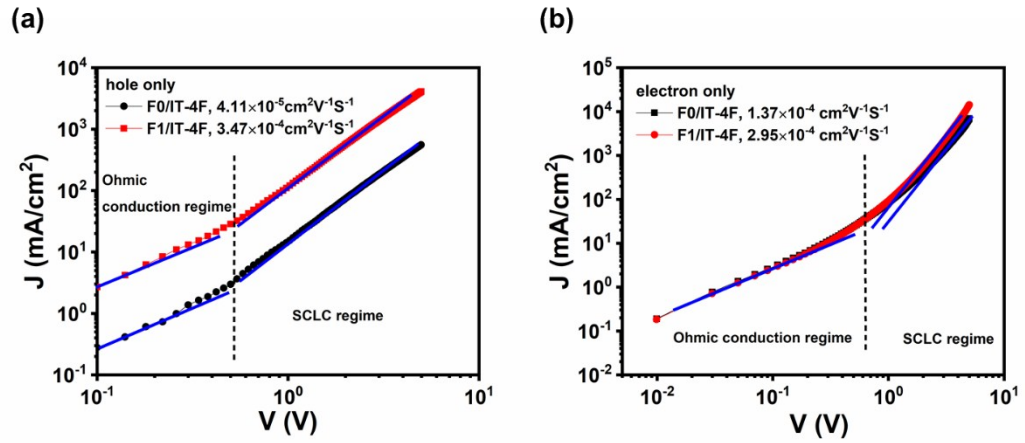

Figure S4. (a) The hole mobility and (b) the electron mobility of the corresponding devices films measured by SCLC method.

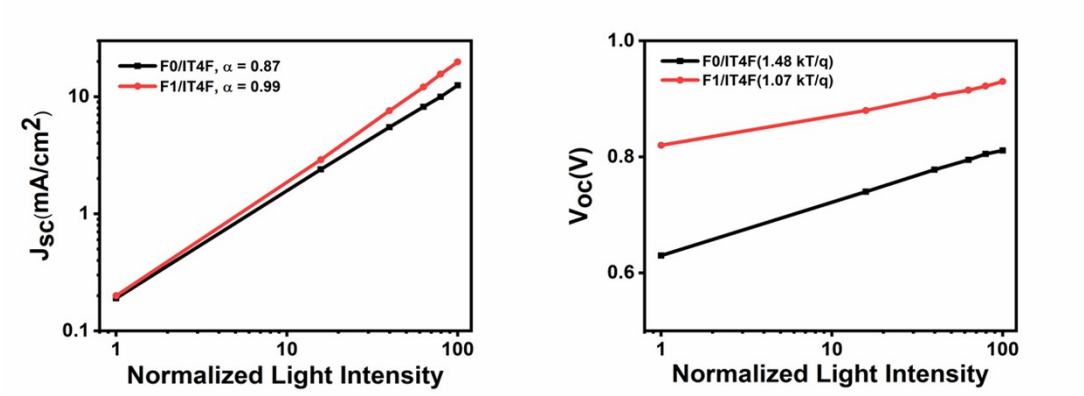

Figure S5. Plots of V_{oc} and J_{sc} versus light intensity.

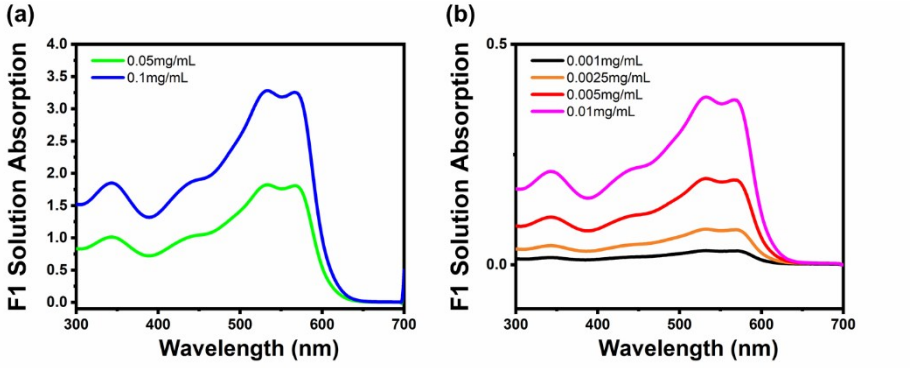

Figure S6. UV-vis absorption curve of F1 in chlorobenzene with different concentration.

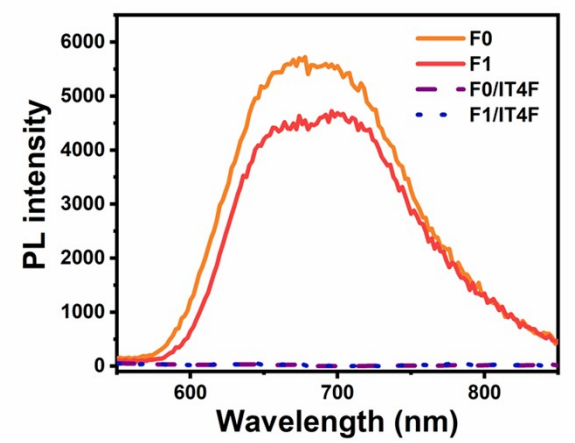

Figure S7. PL spectra of neat polymer films and blends; the samples were excited at 500 nm.

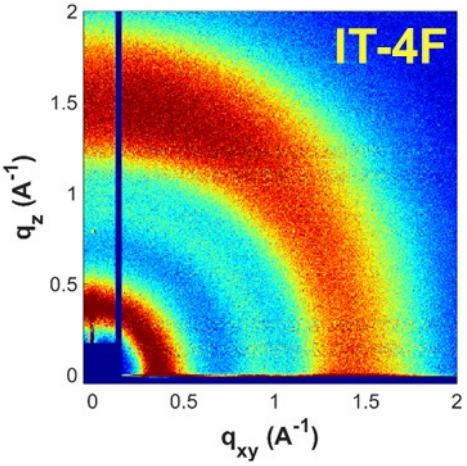

Figure S8. Two-dimensional GIWAXS images of IT-4F films.

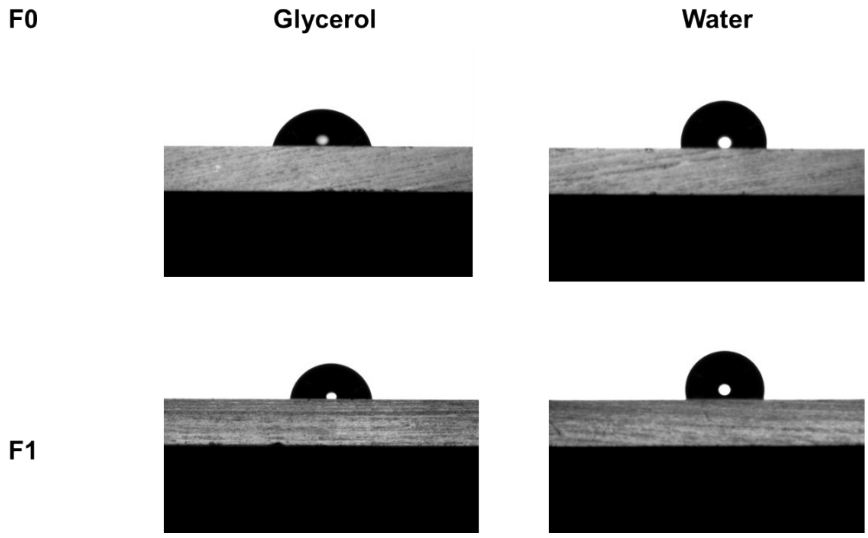

Figure S9. Contact angle of water and glycerol on F0 and F1 films

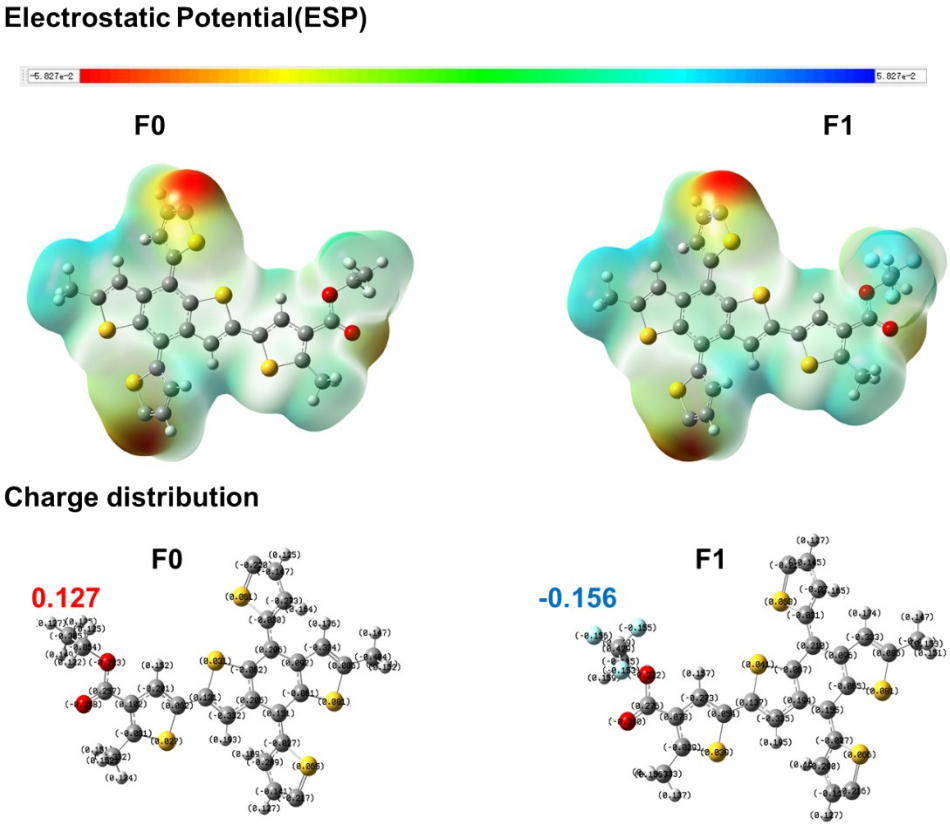

Figure S10. Electrostatic potential (ESP) and charge distributions in F0 and F1.

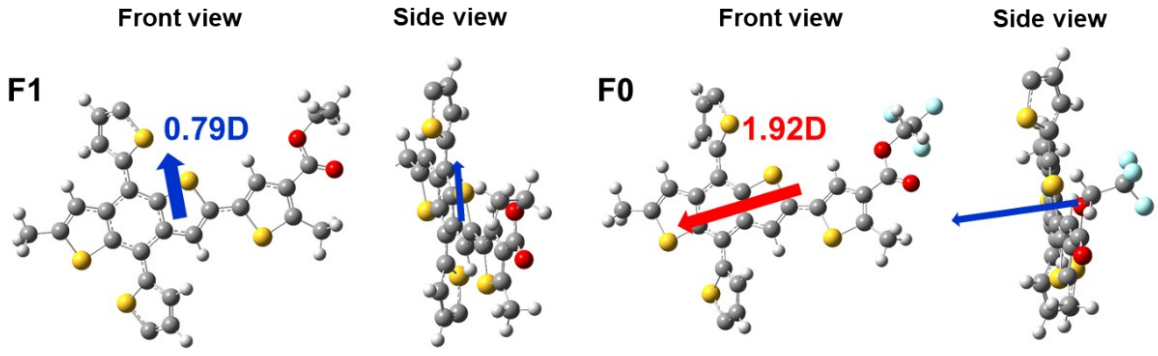

Figure S11. Calculated dipole magnitude and direction of F0 and F1 in side view/front view.

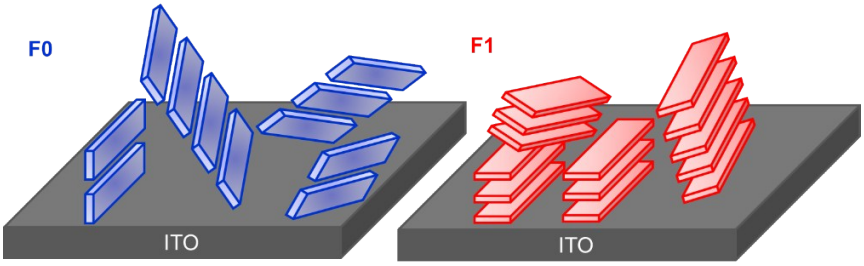

Figure S12. Diagram for polymer aggregation orientation.

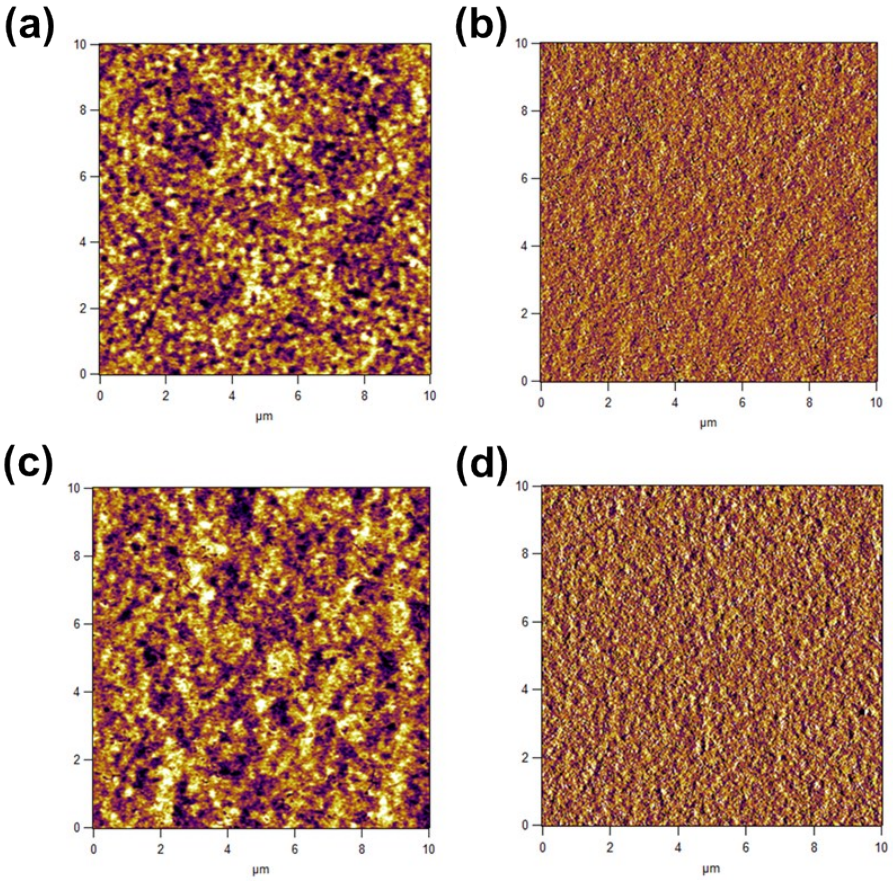

Figure S13.AFM height and phase images of (a)(b)F0, (c)(d)F1.

According to atomic force microscopy (AFM) patterns, the F0/IT-4F and F1/IT-4F blend films

exhibit a root-mean-square surface roughness (R_q) of 0.8 nm and 1.4 nm, respectively.

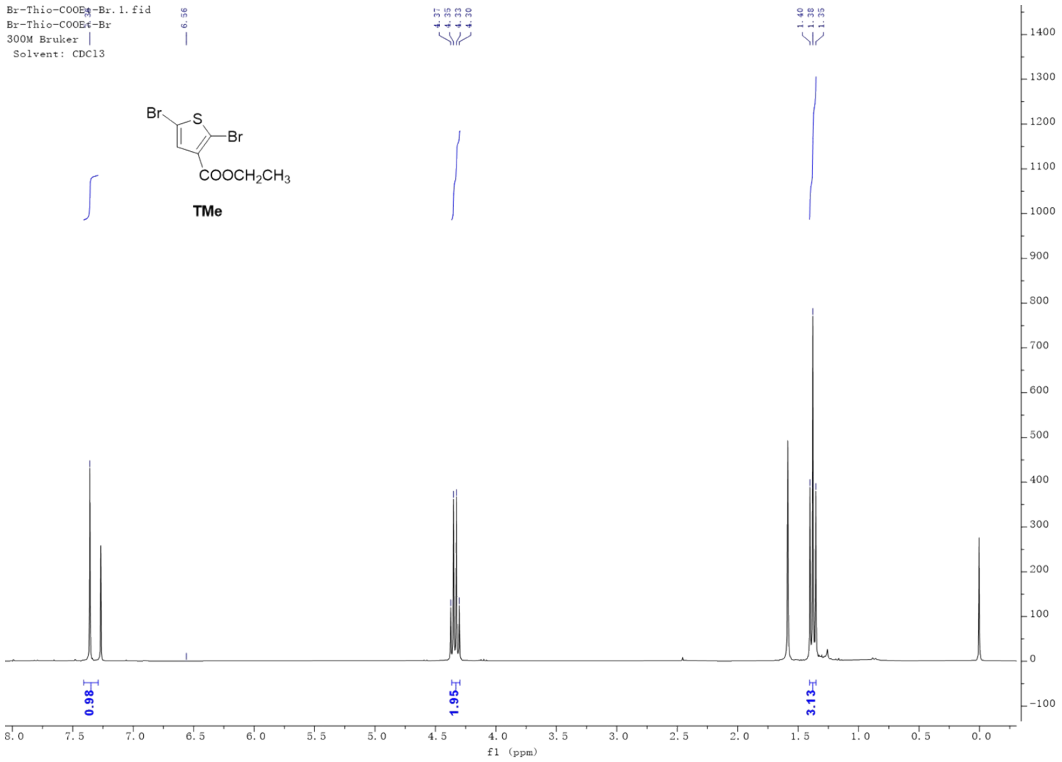

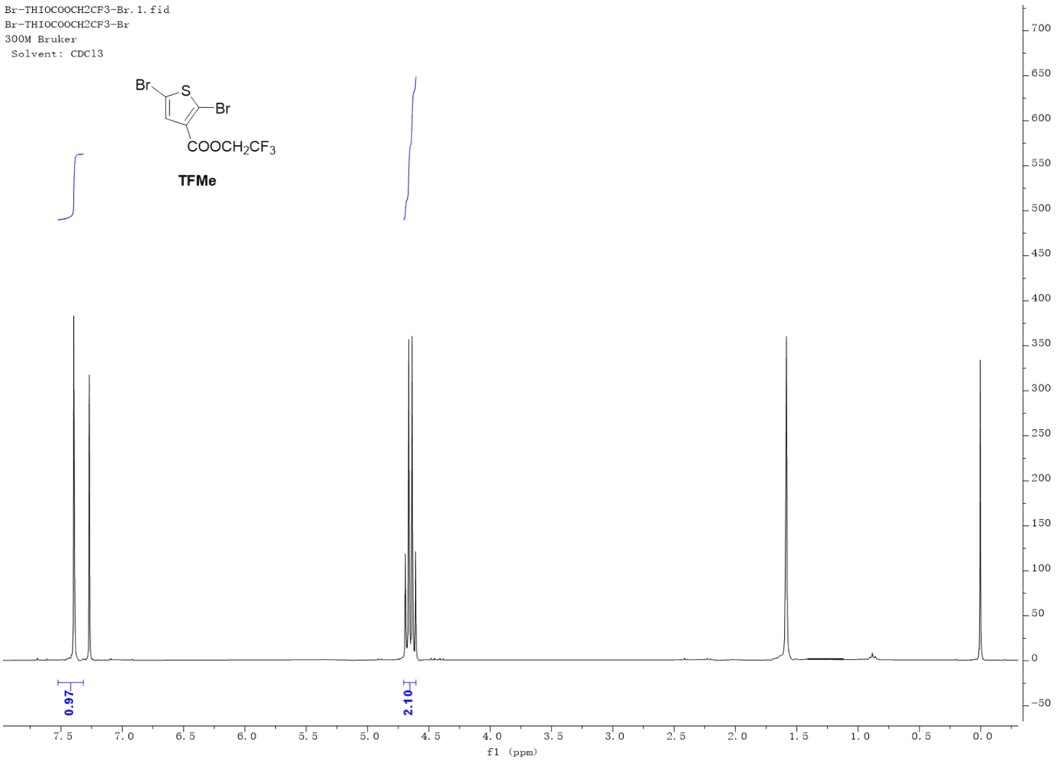

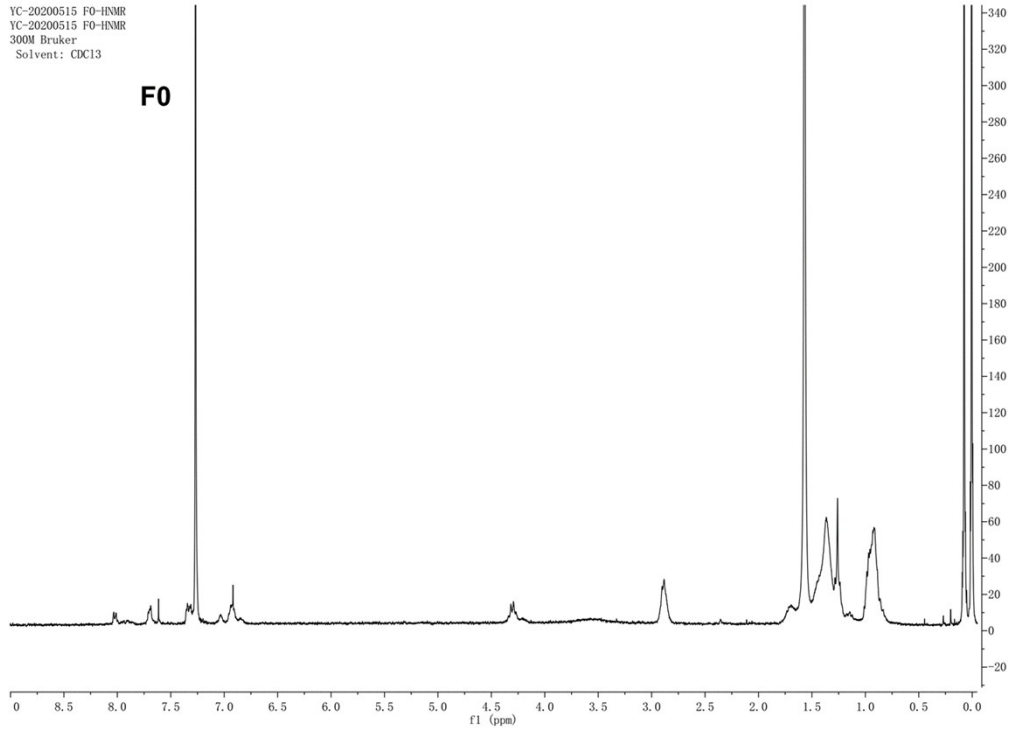
YC-20200515 F0-HNMR
YC-20200515 F0-HNMR
300M Bruker
Solvent: CDCl3
F0
f1 (ppm)

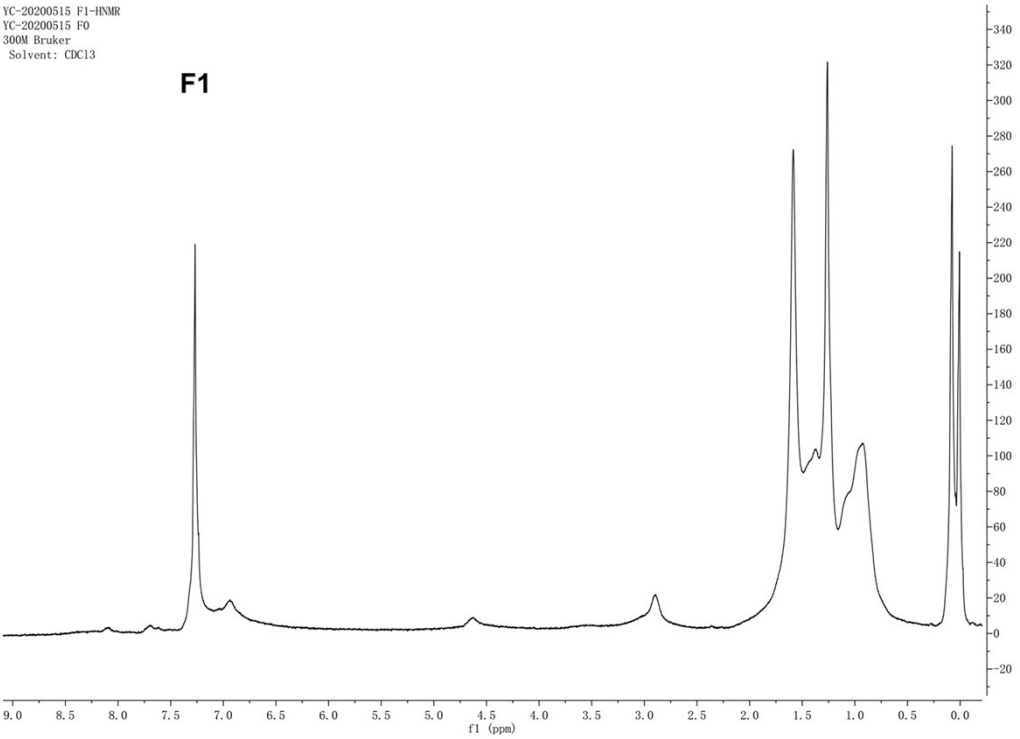
YC-20200515 F1-HNMR
YC-20200515 F0
300M Bruker
Solvent: CDCl3
F1
f1 (ppm)

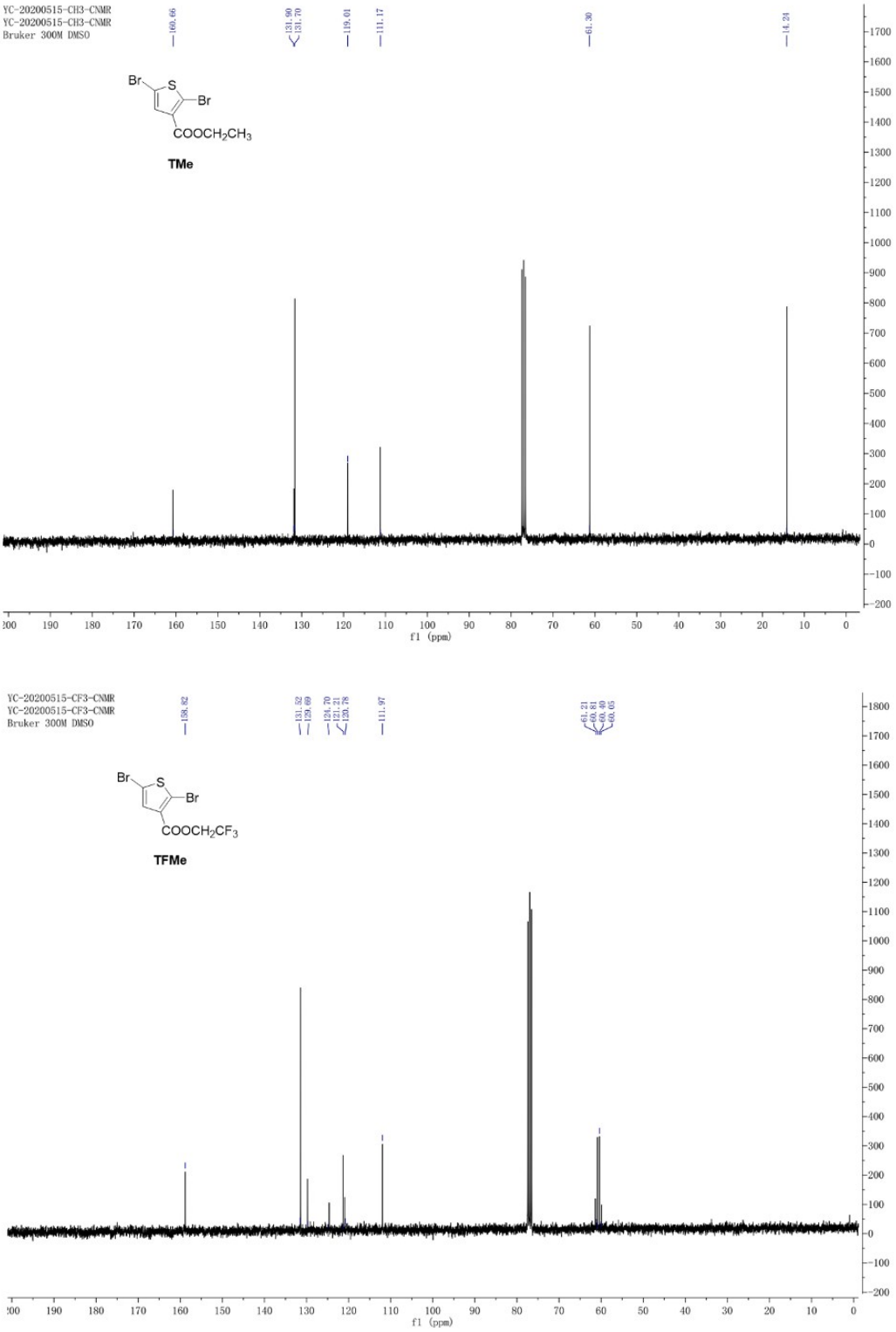

Figure S14.H-NMR spectrum of TMe, TFMe, F0 and F1; C-NMR spectrum of TMe, TFMe.

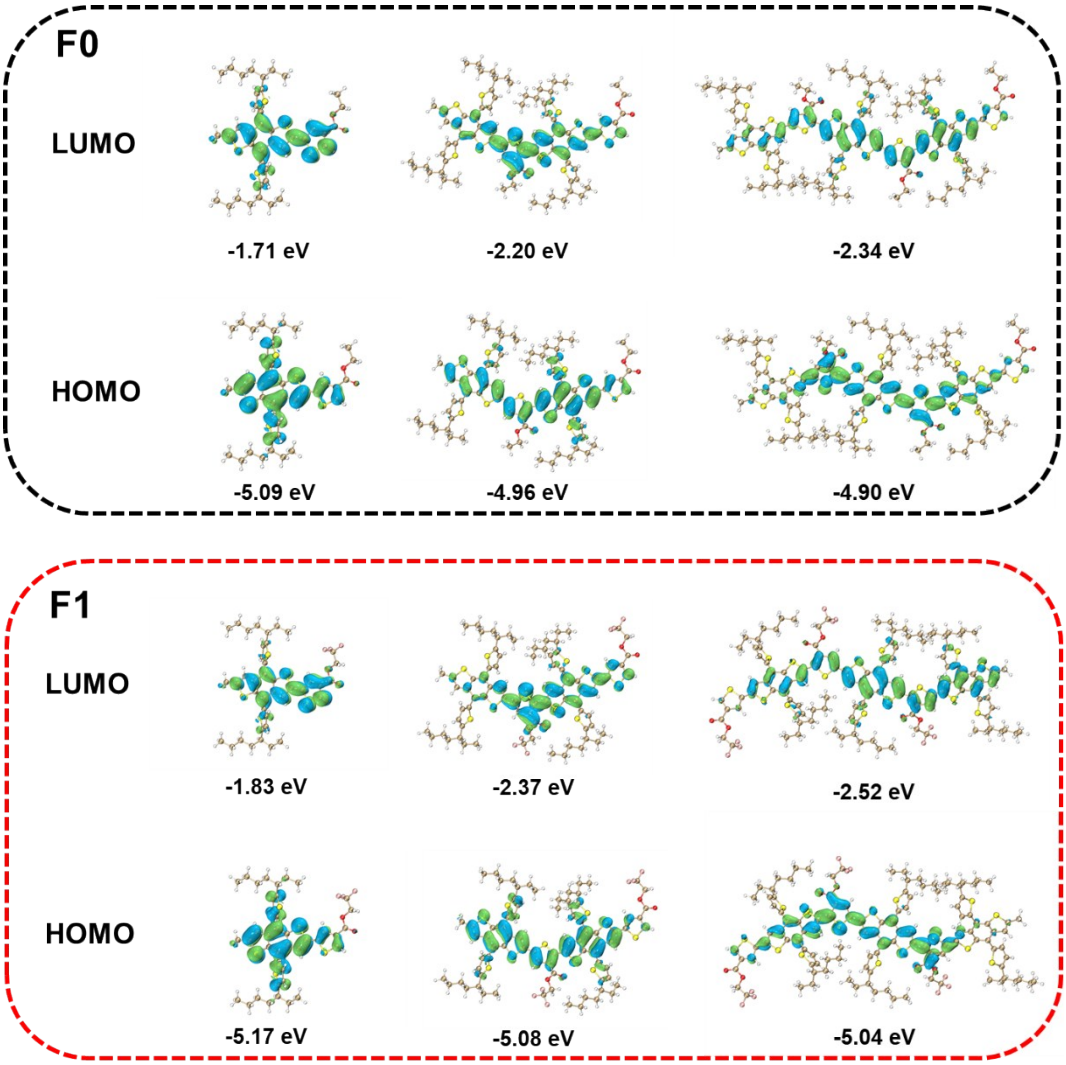

Figure S15. Calculated molecular energy levels of F0 and F1.

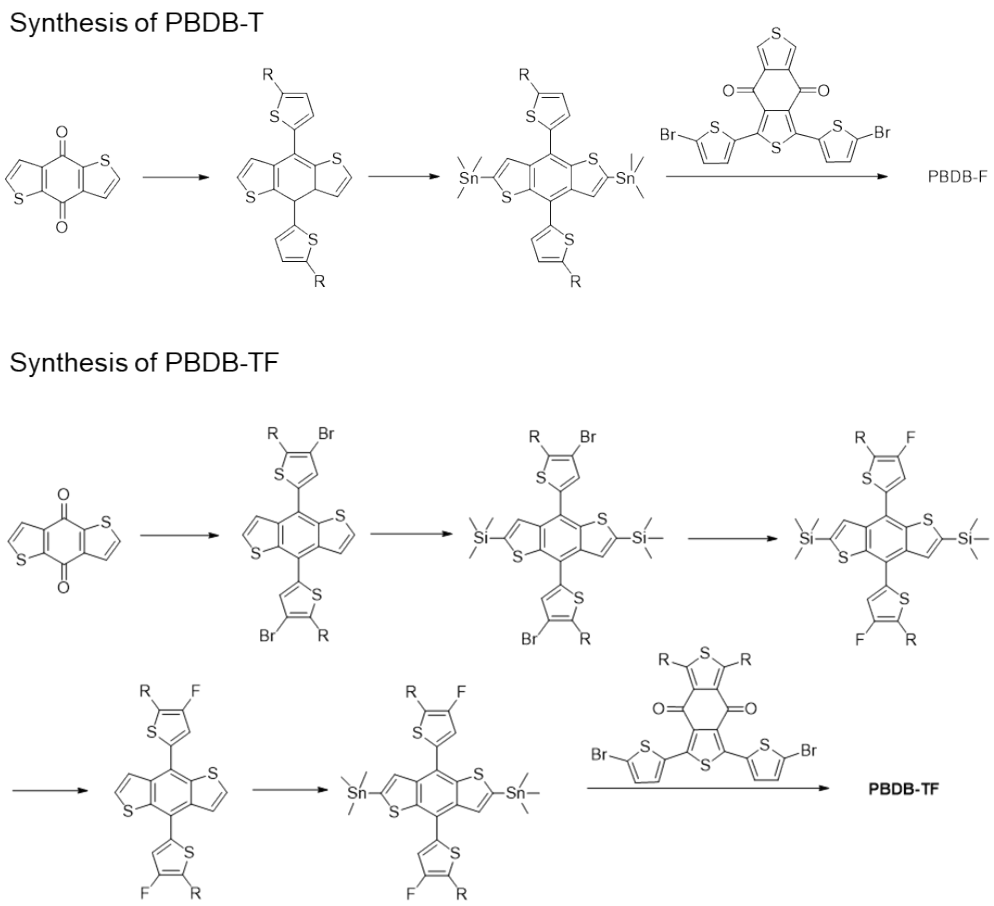

Figure S16. Synthesis route of PBDB-T and PBDB-TF.

Table S1. Device performance under different D/A ratios of (F1/IT-4F).

D/A	V_{oc}(V)	J_{sc}(mA/cm^2)	FF(%)	PCE(%)
1.5/1	0.982 (0.981±0.002)	18.6 (18.5±0.3)	61.4 (61.1±0.5)	11.1 (10.9±0.3)
1/1	0.963 (0.962±0.004)	19.4 (19.0±0.4)	66.5 (66.3±0.3)	12.3 (12.1±0.2)
1/1.5	0.881 ((0.882±0.001))	18.4 (18.2±0.3)	63.2 (62.8±0.5)	10.2 (9.8±0.4)

Table S2. Device performance under different thermal annealing temperature of F1/IT-4F.

T	V_{oc}(V)	J_{sc}(mA/cm^2)	FF(%)	PCE(%)
RT	0.963 (0.961±0.002)	19.4 (19.0±0.4)	66.5 (66.3±0.3)	12.3 (12.1±0.2)

90 ℃	0.944 (0.940±0.004)	19.5 (19.3±0.3)	67.2 (66.8±0.5)	12.3 (12.1±0.3)
120 ℃	0.941 (0.940±0.002)	19.8 (19.6±0.4)	67.4 (67.2±0.3)	12.5 (12.3±0.3)
150 ℃	0.925 (0.921±0.006)	19.6 (19.4±0.2)	66.1 (65.8±0.4)	11.9 (11.7±0.4)

Table S3. Device performance under different DIO concentration of F1/IT-4F.

DIO	**V_{oc}(V)**	**J_{sc}(mA/cm^2)**	**FF(%)**	**PCE(%)**
0	0.944 (0.940±0.006)	19.8 (19.5±0.4)	67.1 (66.8±0.4)	12.5 (12.3±0.3)
0.25%	0.932 (0.932±0.002)	20.1 (19.9±0.3)	68.3 (67.9±0.4)	12.7 (12.7±0.2)
0.5%	0.930 (0.929±0.003)	20.6 (20.4±0.3)	70.2 (70.1±0.3)	13.5 (13.2±0.3)
1%	0.894 (0.892±0.006)	19.1 (19.0±0.3)	65.4 (65.1±0.4)	11.1 (10.9±0.3)

Table S4. Device performance under different D/A ratios of (F0/IT-4F).

D/A	**V_{oc}(V)**	**J_{sc}(mA/cm^2)**	**FF(%)**	**PCE(%)**
1.5/1	0.851 (0.848 ± 0.007)	12.6 (12.3 ± 0.4)	41.2 (39.8 ± 0.6)	4.1 (4.0 ± 0.3)
1/1	0.832 (0.830 ± 0.004)	13.5 (13.4 ± 0.2)	44.1 (44.0 ± 0.4)	4.9 (4.6 ± 0.3)
1/1.5	0.815 (0.814 ± 0.004)	13.2 (13.0 ± 0.3)	38.5 (39.1 ± 0.7)	3.9 (3.9 ± 0.3)

Table S5. Device performance under different thermal annealing temperature of F0/IT-4F.

T	**V_{oc}(V)**	**J_{sc}(mA/cm^2)**	**FF(%)**	**PCE(%)**
RT	0.844 (0.841 ± 0.005)	13.1 (13.0 ± 0.2)	43.2 (42.8 ± 0.5)	4.5 (4.3 ± 0.2)

90 ℃	0.832 (0.830 ± 0.004)	13.5 (13.4 ± 0.2)	44.1 (44.0 ± 0.4)	4.9 (4.6 ± 0.3)
120 ℃	0.824 (0.822 ± 0.003)	12.6 (12.7 ± 0.1)	42.4 (42.2 ± 0.5)	3.8 (3.4 ± 0.5)
150 ℃	0.788 (0.771 ± 0.015)	11.1 (11.0 ± 0.2)	38.1 (37.8 ± 0.4)	2.5 (2.3 ± 0.3)

Table S6. Device performance under different DIO concentration of F0/IT-4F.

DIO	**V_{oc}(V)**	**J_{sc}(mA/cm^2)**	**FF(%)**	**PCE(%)**
0	0.844 (0.841 ± 0.005)	13.1 (13.0 ± 0.2)	43.2 (42.8 ± 0.5)	4.5 (4.3 ± 0.2)
0.25%	0.832 (0.832±0.002)	13.5 (13.4±0.3)	44.3 (43.9±0.4)	4.8 (4.7±0.2)
0.5%	0.823 (0.819±0.004)	11.7 (11.6±0.4)	41.3 (40.9±0.4)	4.1 (4.0±0.2)
1%	0.804 (0.802±0.006)	10.1 (10.0±0.3)	35.4 (35.1±0.6)	2.3 (2.2±0.3)

Table S7. Calculated dipole moment magnitude and direction values of F0 and F1

Polymer	μ_x (Debye)	μ_y (Debye)	μ_z (Debye)	μ (Debye)
F0	-0.0842	0.7928	-0.0104	0.7984
F1	1.2552	-0.2538	-1.4263	1.9168

1. Pomerantz, M., H. Yang, and Y. Cheng, *Poly(alkyl thiophene-3-carboxylates). Synthesis and Characterization of Polythiophenes with a Carbonyl Group Directly Attached to the Ring.* Macromolecules, 1995. **28**(17): p. 5706-5708.
2. Hait, D. and M. Head-Gordon, *How Accurate Is Density Functional Theory at Predicting Dipole Moments? An Assessment Using a New Database of 200 Benchmark Values.* Journal of Chemical Theory and Computation, 2018. **14**(4): p. 1969-1981.